Atomic force microscopy of height fluctuations of fibroblast cells

Bálint Szabó and Dávid Selmeczi
Department of Biological Physics, Eötvös University, Budapest, Hungary

Zsuzsanna Környei and Emília Madarász
Institute of Experimental Medicine, Budapest, Szigony u. 43, Hungary

Noémi Rozlosnik
Department of Biological Physics, Eötvös University, Budapest, Pázmány Péter sétány 1/A, 1117 Hungary
(Received 1 October 2001; revised manuscript received 18 December 2001; published 28 March 2002)

We investigated the nanometer scale height fluctuations of 3T3 fibroblast cells with the atomic force microscope under physiological conditions. A correlation between these fluctuations and lateral cellular motility can be observed. Fluctuations measured on leading edges appear to be predominantly related to actin polymerization-depolymerization processes. We found fast (5 Hz) pulsatory behavior with 1–2 nm amplitude on a cell with low motility showing emphasized structure of stress fibers. Myosin driven contractions of stress fibers are thought to induce this pulsation.

DOI: 10.1103/PhysRevE.65.041910 PACS number(s): 87.64.Dz, 87.17.Jj, 87.16.Nn

I. INTRODUCTION

The motility of animal cells is dominated by actin-myosin-based contraction and actin polymerization-based protrusion. The two basic types of protrusions, lamellipodia and filopodia are driven by actin polymerization-depolymerization processes [1–3]. The physical theory of such biological motilities employing the tools of statistical physics [4,5] gives an idea how it works but it still needs to be developed.

A number of cellular activities can cause height fluctuations on the time and distance scales that we investigated. Actin polymerization and actin-myosin-based contractions represent only one class. The rearrangement of the structure built up from intermediate filaments (IF) under the plasma membrane can be another source of vertical fluctuations. IFs provide mechanical stability to animal cells. Any significant weakening of the IF array alters at least locally the elastic properties of the cell leading to increased susceptibility to intrinsic or extrinsic forces. Assembly or disassembly of large protein complexes in the plasma membrane or their lateral motion under the atomic force microscope (AFM) tip will also result in vertical motility, not to mention the endocytotic and exocytotic activities. Intracellular transport processes can have an effect on the vertical fluctuations, as well.

Cellular motility on the micrometer scale has been extensively investigated with video microscopy ([6–8] and references therein). Spatial resolution provided by optical microscopy of living cells, however, does not enable researchers to observe nanometer scale motion and rearrangement of cell components. AFM is an adequate tool for such measurements [9–12]. Stress fibers (contractile bundles of actin filaments and myosin-II) play an important role in the control of the cell shape and the adhesion of cells to the extracellular matrix through focal contacts. These characteristic cytoskeletal elements can be imaged with the AFM due to their high elastic modulus [13,14]. AFM is capable not only for recording high-resolution topographic images of living cells, but also for measuring the elastic properties of them simultaneously [15] and investigating cellular dynamics [16,17].

By repetitively scanning on the surface of a cell, time-lapse images can be recorded [18,19]. The analysis of subsequent images yielding a movie is highly informative in terms of the kinetics of the cytoskeleton. Although fast cellular motility cannot be examined by the repetitive scanning procedure due to the minute range of scanning time, nanometer scale fast motion can be probed by positioning the tip on the area of interest. In this way vertical fluctuations can be investigated almost without a limitation of the time scale.

Close to the molecular scale the motion of cells is dominated by stochastic fluctuations. Using the AFM we tried to shed light on the linkage between microscopic fluctuations and organized motility.

II. MATERIALS AND METHODS

A. Cell culture

3T3 mouse fibroblasts were cultured in DMEM supplemented with 10% fetal calf serum (GIBCO), 100 units/ml penicillin G, 0.1 mg/ml streptomycin, and 0.75 μg/ml Amphotericin *B* (SIGMA) at 37 °C, in a 5% CO_2 atmosphere. A few days before AFM measurements cells were subcultured on 13-mm glass cover slips.

B. Atomic force microscopy

We investigated the nanometer scale motion of 3T3 mouse fibroblast cells in culture. Different cells (*C*6 rat glioma) giving similar—unpublished—results were also examined.

A commercial AFM (TopoMetrix Explorer, Santa Clara, CA) with custom-made sample heating control system and fluid chamber was used. Measurements were carried out at 37 °C in CO_2 independent medium containing 10% fetal calf serum (GIBCO). We used soft silicon nitride cantilevers (Thermomicroscopes, Coated Sharp Microlevers, Model No.

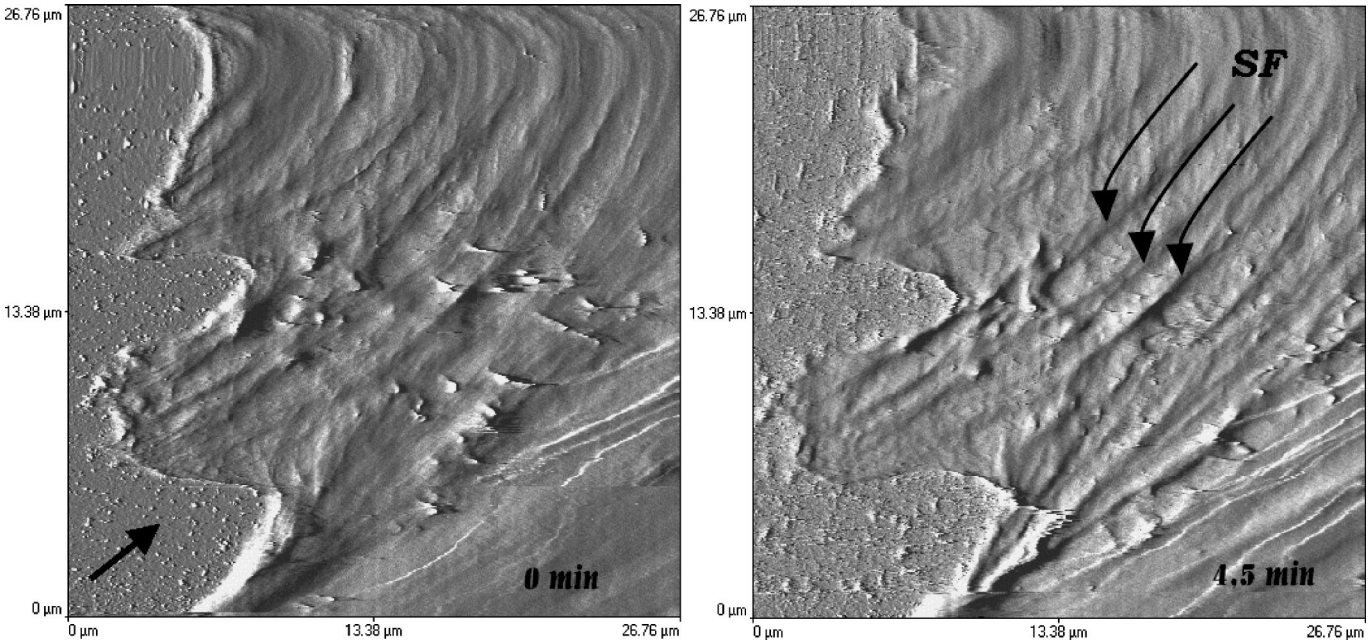

FIG. 1. Shaded deflection mode images with a 4.5-min difference showing stable actin-myosin cables at the rear of a quiescent cell. Arrow in the lower left corner indicates the direction of motion. SF: stress fibers.

MSCT-AUHW, with typical force constant 0.01–0.03 N/m, 20 nm radius of curvature). Topographic and deflection images were acquired in contact mode. High-resolution images were acquired at a scanning frequency of ~4 Hz. Nondestructive low force scanning provided stable sustained imaging of living cells for 8–10 h. After AFM experiments cells were maintained in the same medium for 1–2 days and found to be normal. We could not achieve high-resolution imaging on a portion of cells due to their increased height or softness.

Considering that small details of cellular components can be observed at the best quality on shaded deflection mode images, we present our experimental data in this format. The topographic images provide height information but with a poor contrast.

On the basis of consecutive images local lateral velocity of cells was calculated. At the edges of cells we measured the average displacement of the contour. In the middle of cells we chose some structures with a characteristic shape and the lateral displacements of these structures were measured.

The measurement of local height fluctuations of cells was started at least 1/2 h after mounting the sample into the fluid cell. In this way thermal transient effects could be eliminated. After each scanning the tip was positioned onto the point of interest with the same force and feedback parameters and we captured the dc voltage of the *z* piezo by a digital oscilloscope (Tektronix TDS 210) for 22.5 sec with 100 Hz sampling rate.

III. RESULTS

Distinct types of cellular motility could be examined by the measurement of vertical fluctuations. Figure 1 displays two images of a movie showing the slight motility of the rear edge of a cell with a 4.5-min time shift. This cell was almost quiescent during the experiment with a highly stable structure of cytoskeletal fibers and moderate lateral motility. The rear edge is being pulled by the stress fibers: see the parallel set of curved fibers anchored to the edge of the cell. In the same time cell-matrix junctions or nonspecific contacts adhering to the rear of the cell to the support weaken and break. We also observed a typical retracting triangular shaped 20-μm-wide contact (image not shown) of the same cell at the rear edge. The contact was broken a few minutes after recording the vertical fluctuations.

Typical vertical fluctuations registered on these two locations are presented in Fig. 2. We suppose that the apparent difference between vertical fluctuations originates in the different biological activities of the two regions. While the entire region of the cell shown in Fig. 1 was extremely stable with a lateral velocity of about 2 nm/s, the edge beside the retracting triangle-shaped contact moved with a speed of about 11 nm/s.

To analyze height fluctuations we calculated the power spectrum and the height-height correlation function with a maximal $\tau = 5$-s time shift of each $x(t)$ height-time curve

$$y^2(\tau) = \sum_t \frac{[x(t) - x(t+\tau)]^2}{N}, \quad t = i\Delta t, \quad i = 1, \ldots, N, \tag{1}$$

$$N\Delta t = 22.5 - 5 \text{ s}, \tag{2}$$

where Δt (10 ms) is the sampling time.

This function can characterize stochastic height fluctuations by giving the average change of height as a function of

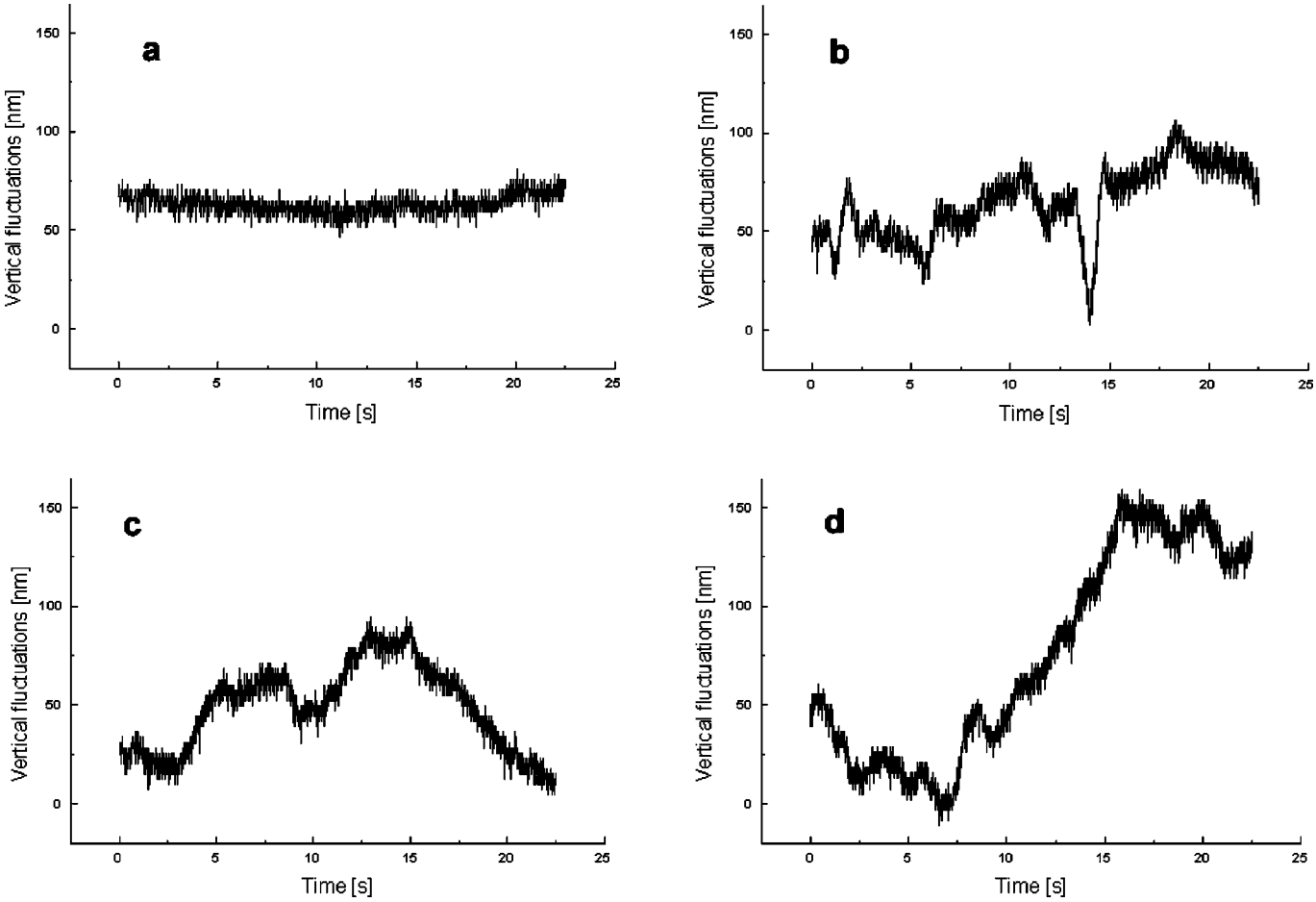

FIG. 2. Typical vertical fluctuations measured on quiescent and motile cells. Graph (a) and (b) belong to the quiescent, (c) and (d) to the motile cell. We recorded (a) on the rear edge displayed in Fig. 1. (b) was measured on a typical retracting triangle shaped contact (image not shown) of the cell at the rear edge. This contact to the support was broken a few minutes after recording the vertical fluctuations. (c) and (d) were registered on the leading edge shown in Fig. 5 and close to that on the cell body, respectively.

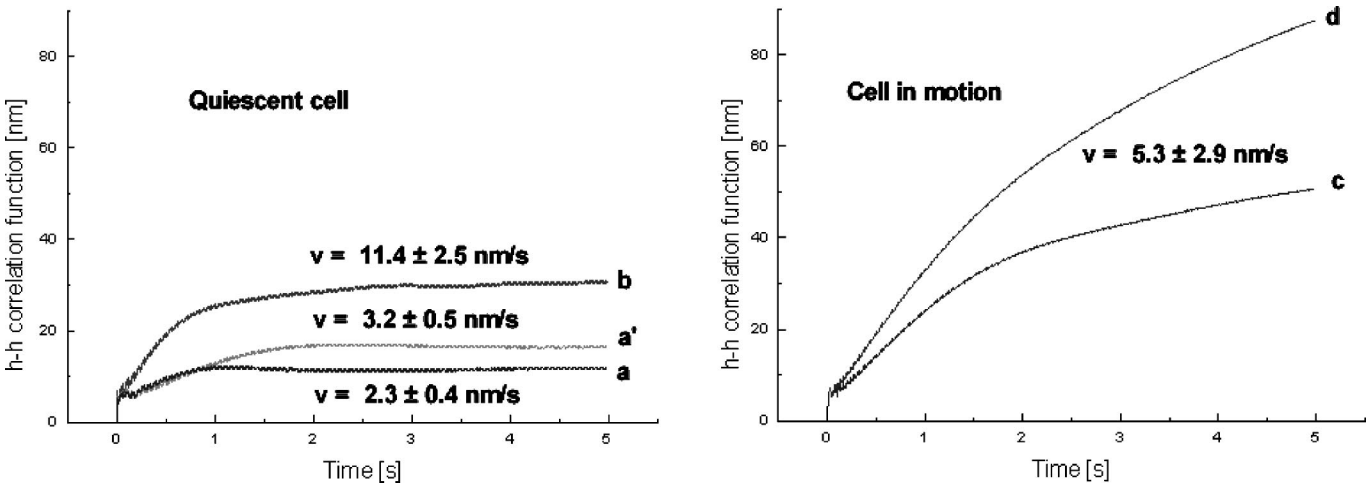

FIG. 3. Averaged height-height correlation functions of fluctuations measured on the surface of the quiescent and the motile cell. Curves $(a,n=10)$; $(b,n=8)$; $(c,n=10)$; and $(d,n=9)$ are the corresponding correlation functions of vertical fluctuations shown in Fig. 2. Curve $(a',n=10)$ was registered on the middle region of the quiescent cell. There is an apparent difference between the behavior of curves belonging to the quiescent and the motile cell. Saturation disappears on the scale of several seconds in the case of the motile cell. This fact indicates the presence of vertical motility on this time scale. Significant difference between graph (*a*) and (*b*) is attributed to the dynamics of the retracting contact at the rear edge. See the value of lateral velocity of locations at each curve. 50 Hz noise on curves can be observed.

TABLE I. Comparison of the lateral velocity and parameters characterizing vertical fluctuations of different locations on the quiescent and the motile cell. Parameters of the height-height correlation function are calculated on the basis of curves presented in Fig. 3. The starting slope and the saturation value were determined by linear fitting in the (0.3 s, 1 s) and (3 s, 5 s) intervals respectively, r: correlation coefficient of fitting, SD: standard deviation, n: number of measured height-time curves.

Curve		Starting slope (nm/s)	r	Saturation value $\pm$ SD (nm)	n	Lateral velocity $\pm$ SD (nm/s)
Quiescent cell	a	6.3	0.94	10.5 ± 0.2	10	2.3 ± 0.4
	a'	8.4	0.97	17.0 ± 0.2	10	3.2 ± 0.5
	b	16.7	0.97	28.1 ± 0.3	8	11.4 ± 2.5
Cell in motion	a	20.3	0.998		10	5.3 ± 2.9
	b	28.7	0.999		9	5.3 ± 2.9

time. Curves are presented in Fig. 3, the number of measured height-time curves n is indicated. The lateral velocity of each location seems to correlate with the saturation value of the height-height correlation function measured at that location, confirming our assumption that height fluctuations are related to local biological activity (motility). The starting slopes of the curves give the speed of fast fluctuations. Curves saturate with different characteristic (saturation) times. There is an apparent difference between curves (a) and (b) in the saturation value. The characteristic time (~ 2 s) of curve (a') is approximately double than that of the other two curves. Curve (a') was registered on the middle region (cell body) of the quiescent cell (see Table I). The characteristic time and saturation value are related to the average duration and amplitude, respectively, of an upward or downward motion.

The analysis of power spectra (Fig. 4) of the height-time curves acquired on each location of this quiescent cell revealed sustained periodic fluctuations during the experiment (1.5 h). We found a characteristic peak at 4.9 Hz with a width of 3.5 Hz. The area of this peak gives an average amplitude of 1.5 ± 0.4 nm. Cells without apparent stress fibers nearby lack this peak. The origin of the sharp peaks in the spectrum is electric noise.

Figure 5 shows the contours of a leading edge of a motile cell from consecutive images. Note the bright spot S appearing on the cell surface close to the edge in the middle of the second image. It appears in less than 7 min and disappears soon after. A similar spot can be observed on the upper part of the last image. These features seem to be linked to the ends of curved filaments. In many cases micrometer-sized unidentified nodes were found on stress fibers. They might be large protein complexes attached to F-actin.

Figure 2 displays the height-time curves captured on the leading edge (c) and close to that on the cell body (d). Curves show increased motility especially on the long (several seconds) time scale. As a consequence, the saturation effect of the height-height correlation function disappears on this scale (Fig. 3). The speed of the fast fluctuations is higher, as well (see Table I). We suppose that the observed increase in vertical fluctuations is an outcome of actin polymerization-depolymerization processes at the leading edge. Surprisingly, the height-height correlation function shows a higher level of fluctuations farther from the leading edge. It can be a result of actin depolymerization processes well behind the edge or an increased temporal motility of this region that has to follow the edge.

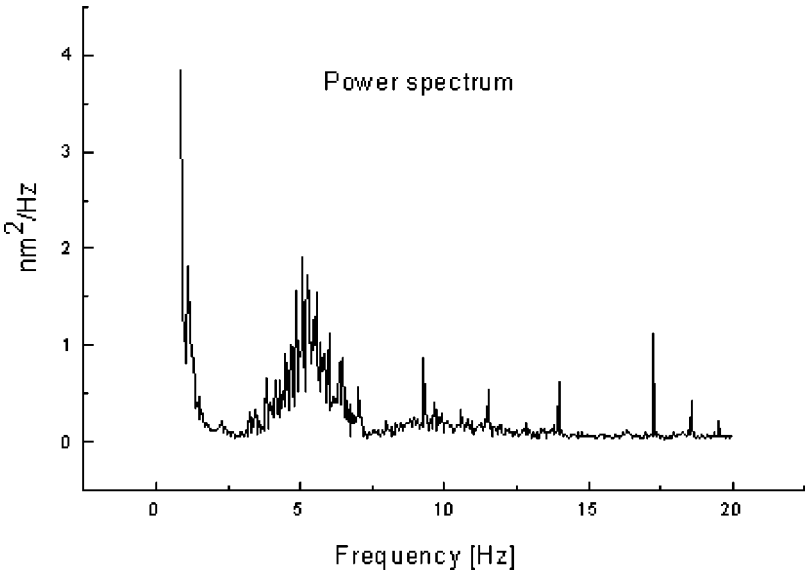

FIG. 4. Power spectrum ($n = 10$) of height fluctuations measured at the location shown in Fig. 1. The peak at 4.9 Hz can be found in each power spectrum of height fluctuations captured on the surface of the quiescent cell. The power spectra of height fluctuations of cells without apparent stress fibers nearby lack this peak.

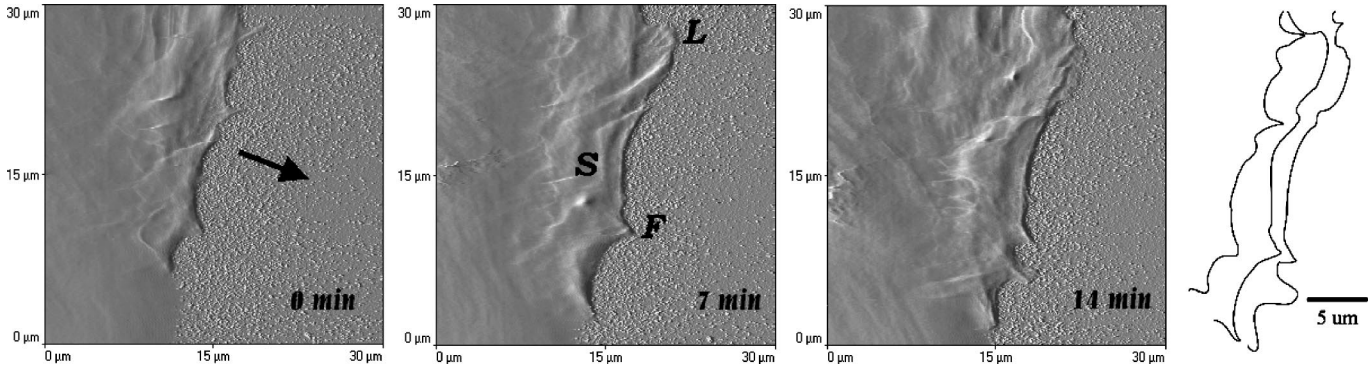

FIG. 5. Consecutive shaded deflection mode images of a leading edge. Approximately 7 min elapsed between images. Arrow indicates the direction of motion. Note the bright spot *S* appearing on the cell surface close to the edge in the middle of the second image. *L*, lamellipodium, *F*, filopodium. Contour lines (extreme right) display the forward motion of the edge. The standard deviation of lateral velocity was found to be higher than in the case of a less mobile edge due to extensions growing with high speed, such as the extension on the lower region of the last contour line corresponding to the right hand image.

IV. DISCUSSION

The analysis of height fluctuations acquired at different locations allows a sensitive monitoring of the motility of cellular components. Both actin-myosin-based contractions and actin polymerization-based filopodial and lamellipodial protrusions can be examined by this method. We found a correlation between the characteristics of vertical fluctuation and organized lateral locomotion.

We explain the observed 5 Hz pulsation of a cell with the periodic contractions of stress fibers. This type of oscillation cannot be easily identified by other techniques due to its low amplitude. Although the frequency of mechanical pulsation of cardiomyocytes is in the same frequency range ($\sim$1.25 Hz), its amplitude is two orders of magnitude higher [16]. Spontaneous oscillatory contractions of muscle fibers with a period of a few seconds are widely known for several years (e.g.. Ref. [20]). Theoretical models can explain spontaneous oscillation under certain conditions [21].

Slow pulsation of nonmuscle cells has been observed in several cases. Microtubule depolymerization can induce rhythmic actomyosin-based contractility with a period of $\sim$50 s in fibroblasts [22] and oscillatory activity in the cortical microfilament system of lymphoblasts [23]. Shape oscillations of leukocytes driven by cyclic actin polymerization has been studied by several groups [24]. The period of this process is about 8 s.

The cortical tension of nonmuscle cells generated by myosin II can drive a change of shape [25]. Myosin molecules cycle about five times in a second in a muscle [26]. Based on the above-mentioned facts, we think that a synchronized behavior of myosin molecules in stress fibers may cause the observed pulsation. Myosin synchronization has been theoretically predicted close to the isometric condition in highly organized actin structures [27,28]. Further experiments are needed to elucidate the background of this phenomenon. Using drugs affecting a specific system of the cytoskeleton will help to distinguish their roles in the nanometer scale fluctuations of cells.

ACKNOWLEDGMENTS

We thank Elöd Méhes, András Czirók, Balázs Hegedös for discussions and help in cell culturing, Jeremy Ramsden for consultation on the presentation of our results, and Imre Derényi for discussions in the field of myosin motors.

[1] L.M. Machesky and A. Hall, J. Cell Biol. **138**, 913 (1997).
[2] H. Chen, B.W. Bernstein, and J.R. Bamburg, TIBS **25**, 19 (2000).
[3] G.G. Borisy and T.M. Svitkina, Curr. Opin. Cell Biol. **12**, 104 (2000).
[4] L. Mahadevan and P. Matsudaira, Science **288**, 95 (2000).
[5] Ch.S. Peskin, G.M. Odell, and G.F. Oster, Biophys. J. **65**, 316 (1993).
[6] A. Czirók, K. Schlett, E. Madarász, and T. Vicsek, Phys. Rev. Lett. **81**, 3038 (1998).
[7] B. Hegedös, A. Czirók, I. Fazekas, T. Bábel, E. Madarász, and T. Vicsek, J. Neurosurg. **92**, 428 (2000).
[8] Zs. Környei, A. Czirók, T. Vicsek, and E. Madarász, J. Neurosci. Res. **61**, 421 (2000).
[9] H.J. Butt, E.K. Wolff, S.A. Gould, B. Dixon Northern, C.M. Peterson, and P.K. Hansma, J. Struct. Biol. **105**, 54 (1990).
[10] E. Henderson, P.G. Haydon, and D.S. Sakaguchi, Science **257**, 1944 (1992).
[11] V. Parpura, P.G. Haydon, and E. Henderson, J. Cell. Sci. **104**, 427 (1993).
[12] Ch. Rotsch, K. Jacobson, and M. Radmacher, Proc. Natl. Acad. Sci. U.S.A. **96**, 921 (1999).
[13] C. Rotsch and M. Radmacher, Biophys. J. **78**, 520 (2000).
[14] U.G. Hofmann, C. Rotsch, W.J. Parak, and M. Radmacher, J. Struct. Biol. **119**, 84 (1997).
[15] M. Lekka, P. Laidler, D. Gil, J. Lekki, Z. Stachura, and A.Z. Hrynkiewicz, Eur. Biophys. J. **28**, 312 (1999).
[16] J. Domke, W.J. Parak, M. George, H.E. Gaub, and M. Radmacher, Eur. Biophys. J. **28**, 179 (1999).
[17] S.W. Schneider, K.C. Sritharan, J.P. Geibel, H. Oberleithner,

and B.P. Jena, Proc. Natl. Acad. Sci. U.S.A. **94**, 316 (1997).
[18] H. Haga, M. Nagayama, K. Kawabata, E. Ito, T. Ushiki, and T. Sambongi, J. Electron Microsc. **49**, 473 (2000).
[19] C.A. Shönenberger and J.H. Hoh, Biophys. J. **67**, 929 (1994).
[20] K. Yasuda, Y. Shindo, and S. Ishiwata, Biophys. J. **70**, 1823 (1996).
[21] F. Jülicher, A. Ajdari, and J. Prost, Rev. Mod. Phys. **69**, 1269 (1997).
[22] O.J. Pletjushkina, Z. Rajfur, P. Pomorski, T.N. Oliver, J.M. Vasiliev, and K.A. Jacobson, Cell Motil. Cytoskeleton **48**, 235 (2001).
[23] M. Bornens, M. Paintrand, and C. Celati, J. Cell. Biol. **109**, 1071 (1989).
[24] M.U. Ehrengruber, D.A. Deranleau, and T.D. Coates, J. Exp. Biol. **199**, 741 (1996).
[25] C. Pasternak, J.A. Spudich, and E.L. Elson, Nature (London) **341**, 549 (1989).
[26] B. Alberts, D. Bray, J. Lewis, M. Raff, K. Roberts, and J.D. Watson, *Molecular Biology of the Cell*, 3rd ed. (Garland Publishing, New York, 1994), p. 853.
[27] T.A.J. Duke, Proc. Natl. Acad. Sci. U.S.A. **96**, 2770 (1999).
[28] T. Duke, Trans. R. Soc. Lond. B Biol. Sci. **355**, 529 (2000).